




Inhibiting Effect of Zinc Oxide Nanoparticles on Advanced Glycation Products and Oxidative Modifications: a Potential Tool to Counteract Oxidative Stress in Neurodegenerative Diseases

Jalaluddin M. Ashraf¹ · Mohammad Azam Ansari² · Sana Fatma³ · Saleh M. S. Abdullah¹ · Johar Iqbal⁴ · Aymen Madkhali¹ · Al Hassan Hamali¹ · Saheem Ahmad⁵ · Ahmed Jerah¹ · Valentina Echeverria⁶ · George E. Barreto⁷  · Ghulam Md Ashraf⁸

Received: 20 November 2017 / Accepted: 25 January 2018 / Published online: 8 February 2018
© Springer Science+Business Media, LLC, part of Springer Nature 2018

Abstract

Advanced glycation end products (AGEs) are implicated in several central nervous system (CNS) pathologies including Alzheimer and Parkinson's diseases. In the face-off of AGE menace, we have attempted to investigate the zinc oxide nanoparticle (ZnONP) role in inhibition of AGE formation. Synthesized ZnONPs were used to investigate the inhibitory effects on AGE formation. The inhibitory effects of ZnONPs on AGE formation were determined by biophysical immunological and biochemical techniques. The results showed that ZnONP is a potential anti-glycating agent inhibiting AGE formation as well as protecting the protein structure from change. Therefore, our findings suggest ZnONPs may be used as a therapeutic in resolving the AGE role in CNS-related complications.

Keywords Advanced glycation end products · Anti-glycating agent · Neurodegenerative diseases · Nanoparticles

Introduction

The non-enzymatic glycation named Maillard reaction is an unavoidable phenomenon even under physiological condition resulting in advanced glycation end products (AGEs). It is now well established that long-term exposure of macromolecules during metabolic dysfunction and/or other diseased conditions (specifically neurodegenerative events) drastically increases non-enzymatic glycation reaction and eventually leads to AGE accumulation [1–4]. Increasing evidence suggests that

excessive formation of oxidative stress and accumulation of AGEs in the body result in oxidative and carbonyl stress, inflammation, and structural and functional changes of tissue proteins, as a consequence of Alzheimer's disease (AD) and Parkinson's disease (PD) [1, 5].

Previously, it was considered that only reducing sugars were involved in glycation reaction, i.e., AGE formation, but later, several other non-sugar compounds were also reported to be indulged in glycation reactions [6, 7]. α -Dicarbonyl species (methylglyoxal (MG), glyoxal (G), and 3-deoxyglucosone

Jalaluddin M. Ashraf and Mohammad Azam Ansari are equally contributing authors

✉ Jalaluddin M. Ashraf
jmashraf@gmail.com

✉ Mohammad Azam Ansari
azammicro@gmail.com; maansari@iau.edu.sa

✉ Ghulam Md Ashraf
ashraf.gm@gmail.com

¹ Faculty of Applied Medical Sciences, Jazan University, Jazan, Saudi Arabia

² Department of Epidemic Disease Research, Institute of Research and Medical Consultations (IRMC), Imam Abdulrahman Bin Faisal University, Dammam 31441, Saudi Arabia

³ Institute of Science, Banaras Hindu University, Varanasi, India

⁴ Faculty of Medicine, Jazan University, Jazan, Saudi Arabia

⁵ Department of Biosciences, Integral University, Lucknow, India

⁶ Facultad de Ciencias de la Salud, Universidad San Sebastián, Lientur 1457, 4030000 Concepción, Chile

⁷ Departamento de Nutrición y Bioquímica, Facultad de Ciencias, Pontificia Universidad Javeriana, Bogotá D.C., Colombia

⁸ King Fahd Medical Research Center, King Abdulaziz University, Jeddah, Saudi Arabia

(3-DG)) endogenously originate from several pathways including Maillard reaction, auto-oxidation of sugars, amino acid metabolism, and lipid peroxidation [8]. These compounds are highly reactive (20,000-fold as reactive as glucose) that promptly glycates biomolecules resulting in rapid formation of AGE even at extremely low concentration [9]. Moreover, a direct link between free radicals generation and MG toxicity is well known and commonly reported in neurodegenerative diseases [10–12]. For example, elevated MG in AD are considered as one of the key factors in the glycation of biomolecules [13]. The long-lived proteins are highly susceptible to glycation [14]. The human immunoglobulin G (IgG) is the most abundant and extensively distributed (about 75–80%) body's total antibody content [15]. Long biological half-life (20–24 days) as well as lysine-rich content makes it a potential target for glycation. Several studies have demonstrated the extent of glycation of IgG and its influence on the biological functionality, after all affecting its overall immunocompetence [16, 17].

Hence, developing pharmacological agents that suppress the notorious AGE formation may be one of the optimistic therapeutic advances for aversion of age-related diseases [18]. In this respect, several compounds, including aminoguanidine, aspirin, and steroidal molecules have been discerned with promising results in reduction of AGEs in neurological diseases [19–22]. Currently, phytochemical compounds (phenols, flavonoids) from dietary plants [23, 24] and herbal medicines [25, 26] have been introduced as AGE inhibitors. Although many of these compounds carry promising anti-glycating property, their utilization was severely limited due to accompanying adverse effects. For example, aminoguanidine was reported as a powerful AGE inhibitor but later it was withdrawn due to adverse effect reported in phase III clinical trials [27, 28]. Therefore, it is evident that there is desperate call for exploration of novel, potent, and safe anti-glycation agents.

Nanotechnology may provide new and powerful tools for eradicating this menacing problem, due to owing the unique properties of nanomaterials, such as nanosize, good biocompatibility, and versatile conjugation with biomolecules [29]. More significantly, nanoparticles can unprecedentedly interact with biomolecules on both the surface and inside cells due to their small size (about 100 to 10,000 times smaller than human cells). Up to now, only a few studies about the inhibitory effect of nanoparticles on protein glycation have been performed. It has been reported that several nanoparticles such as gold, silver, and selenium nanoparticles have capability of attenuating the non-enzymatic glycation of proteins as well as acted as antioxidant [30, 31]. It is known that oxidative stress is one of the factors responsible for causing certain diseases, e.g., in initiation and progression of neurodegenerative diseases [23, 24, 32–35]. Zinc (Zn) is an essential micronutrient and an efficient antioxidant, which has been suggested to have

therapeutic potential [36–39]. Moreover, recent study has demonstrated that Zn(II) exhibited the capability of inhibition of AGE formation [36].

On the basis of available reports about the hazardous role of AGEs in initiation/progression of diseases, we attempted to investigate the role of ZnO nanoparticles (ZnONPs) in attenuating glycation reactions, i.e., AGE formation. In the present study, anti-glycating activity of ZnONPs was verified in MG and human IgG glycation reaction system by employing several physico-chemical techniques. In view of that, these results may offer an important theoretical source for the potential application of ZnONPs as a novel anti-glycation agent.

Materials and Methods

Preparation of the Leaf Extract

ZnONPs were synthesized using aqueous leaf extract of *Aloe vera* plants according to the protocol we have previously reported [6]. Briefly, about 10 g of finely incised leaves was boiled at 80 °C in a 250-ml beakers containing 100 ml distilled water for about 20 min. After cooling, the extracts were centrifuged at 12,000 rpm for 15 min and the supernatants were filtered using a 0.45- μ m PTFE filter and were stored at 4 °C for the green synthesis of ZnONPs.

ZnONPs Synthesis

To synthesize the ZnONPs, an aqueous solution of zinc acetate (1 mM) was used as the precursor. Twenty milliliters of an *Aloe vera* extract was added to 80 ml of 1 mM zinc acetate solution. The reaction mixture was constantly stirred at 60–70 °C for 3 h and then centrifuged at 4500 rpm for 15 min. The creamy colored pellet was collected and washed several times by centrifugation and then dried at 90 °C in an oven for 24 h. The dried ZnONPs were stored in an airtight container and stored for future use.

UV-Vis Spectra Analysis

The formation of ZnONPs was confirmed by spectrophotometric analysis. A preliminary characterization of the green synthesized ZnONPs was carried out using UV-visible spectroscopy (Varian Inc., USA) in the range of 200 to 600 nm.

X-ray Diffraction Analysis

The crystal size and phase of the green synthesized ZnONPs were analyzed using X-ray diffraction (XRD) as described previously [37]. The XRD pattern of ZnONPs was recorded by Bruker D8 diffractometer using $\text{CuK}\alpha$ radiation ($\lambda = 1.54056 \text{ \AA}$) in the range of $20^\circ \leq 2\theta \leq 80^\circ$ at 40 keV. The

particle size (D) of the sample was calculated using the Scherrer's relationship:

$$D = \frac{0.9\lambda}{B \cos \theta} \quad (1)$$

where λ is the wavelength of X-ray, B is the broadening of the diffraction line measured half of its maximum intensity in radians, and θ is the Bragg's diffraction angle [37].

High-Resolution Transmission Electron Microscopy and EDX Analysis of ZnONPs

The morphology and size of the nanoparticles were observed using high-resolution transmission electron microscopy (HR-TEM; Technai G2, FEI, Electron Optics, USA) as described in our previous study [6]. The TEM measurements were performed at an accelerating voltage of 200 kV. The elemental analysis was examined using energy dispersive X-ray spectroscopy (EDX; JED-2300 Japan).

Glycation Reaction System

The glycation reaction system includes IgG, MG as a glycosylating agent, and ZnONPs as an AGE inhibitor as described earlier [7]. Briefly, mixture of IgG (1.5 μ M) and MG (50 μ M) was prepared with or without various concentrations of ZnONPs (25, 50, and 100 μ g/ml) in 0.05 M phosphate buffered saline (PBS, pH 7.4), and then incubated at 37 °C for 6 days. Native IgG (without MG and ZnONPs) was used as a control. After 6 days, the unbound MG and ZnONPs were removed from solutions by dialyzing against sodium phosphate buffer at 4 °C for 48 h.

Determination of Free Amino Groups by Fluorescamine

Mixture of IgG (1.5 μ M) and MG (50 μ M) was prepared with or without various concentrations of ZnONPs (25, 50, and 100 μ g/ml) in 0.05 M phosphate buffered saline (PBS, pH 7.4), and then incubated at 37 °C for 6 days. Screening of lysine side chain modifications was performed using fluorescamine as explained before, with minor amendment [38]. Amino groups form high fluorescent reaction products in this process. First, MG-glycated IgG with or without ZnONPs solution (5 μ l; approx. 1 mg/ml), 100 μ l of 100 mM Na₂HPO₄, 45 μ l distilled water, and 50 μ l fluorescamine reagent (1 mM fluorescamine in acetonitrile) were mixed and incubated for 10 min in the dark in a 96-well plate. The fluorescence of the sample was then measured at excitation/emission wavelengths of 390/490 nm in a FLUORO-STAR plate reader (BMG, Germany). N- α -acetyl-lysine from 0 to 1.5 mM was used to determine the linearity of

fluorescence within the expected lysine content of the protein solution.

Determination of Free Arginine Side Chains by 9,10-Phenanthrenequinone

Mixture of IgG (1.5 μ M) and MG (50 μ M) was prepared with or without various concentrations of ZnONPs (25, 50, and 100 μ g/ml) in 0.05 M phosphate buffered saline (PBS, pH 7.4), and then incubated at 37 °C for 6 days. Analysis of free arginine was performed as earlier described [39]. Briefly, samples (50 μ l) were mixed with 150 μ l of 9,10-phenanthrenequinone reagent (150 μ M in ethanol) and 25 μ l of 2 N NaOH. Protein samples without 9,10-phenanthrenequinone were used to correct the results for AGE fluorescence. Samples were incubated at 60 °C for 3 h, after which 40 μ l was transferred to a 384-well plate and mixed with 40 μ l of 1.2 N HCl. Then, samples were kept in dark at room temperature for 1 h for the development of fluorescence in the reaction product and then a TECAN Safire spectrometer (USA) was used to measure the fluorescence at excitation/emission wavelengths of 312/395 nm. N- α -acetyl-arginine from 0 to 0.4 mM was used to test the linearity of fluorescence within the expected arginine content of the protein solution.

Estimation of Protein-Bound Carbonyl Contents

Mixture of IgG (1.5 μ M) and MG (50 μ M) was prepared with or without various concentrations of ZnONPs (25, 50, and 100 μ g/ml) in 0.05 M phosphate buffered saline (PBS, pH 7.4), and then incubated at 37 °C for 6 days. Determination of carbonyl contents of native and MG-glycated IgG with or without ZnONP samples was carried out as described earlier [40]. Briefly, 15 μ M native and MG-glycated IgG with or without ZnONP samples was added in 10 mM DNPH solution (2,4-dinitrophenyl hydrazine; in 2 N HCl). Samples were then vortexed for 1 h at room temperature (RT) and precipitated with 0.5 ml of 20% (v/v) TCA, followed by centrifugation at 11,000g for 3 min at 4 °C. To remove extra DNPH reagent, pellet was washed with 1 ml of ethanol-ethyl acetic acid mixture (1:1; v/v). Next, samples were incubated at RT for 10 min and then centrifuged at 11,000 \times g for 5 min at 4 °C. The supernatant was discarded and the pellet was washed twice with ethanol-ethyl acetic acid mixture. The protein pellet was then suspended in 1 ml of 6 M guanidinium hydrochloride dissolved in 20 mM potassium phosphate buffer, pH 2.3 (adjusted with trifluoroacetic acid), after which samples were incubated at 37 °C for 15–30 min to make sure complete solubility of proteins. All samples were subsequently centrifuged to get rid of any insoluble material. Carbonyl content was estimated in the supernatant based on the absorbance at 370 nm against 6 M guanidinium hydrochlorides (as blank) using the molar extinction coefficient of

22,000 M⁻¹ cm⁻¹. Protein carbonyl content was expressed as nanomolar per milligram of protein.

Determination of Free Sulfhydryl Groups

Mixture of IgG (1.5 μM) and MG (50 μM) was prepared with or without various concentrations of ZnONPs (25, 50, and 100 μg/ml) in 0.05 M phosphate buffered saline (PBS, pH 7.4), and then incubated at 37 °C for 6 days. Ellman's method was used to estimate the free sulfhydryl groups in native and glycated IgG with or without ZnONP samples [41]. The DTNB (5, 5'-dithio-bis[2-nitrobenzoic acid]) stock and the dilution buffer were prepared as follows: DTNB solution—50 mM sodium acetate (NaAc), 2 mM DTNB in distilled water; Tris solution—1 M Tris/pH 8.0. DTNB stock was diluted in order to prepare the working solution by adding Tris (100 μl) and water (840 μl) in DTNB (50 μl) stock solution. Then, protein (10 μl) samples were added in DTNB (990 μl). It was comprehensively mixed and incubated at 37 °C for 5 min. Absorbance was taken at 412 nm. The free sulfhydryl group content was determined using an extinction coefficient of 13,600 M⁻¹ cm⁻¹.

Estimation of Carboxymethyl Lysine Content by ELISA

Mixture of IgG (1.5 μM) and MG (50 μM) was prepared with or without various concentrations of ZnONPs (25, 50, and 100 μg/ml) in 0.05 M phosphate buffered saline (PBS, pH 7.4), and then incubated at 37 °C for 6 days. Carboxymethyl lysine (CML) content was measured by ELISA as described earlier, with minor modification [34]. Briefly, absorbance was measured at 405 nm using a Model 550 Bio Rad microplate reader. Product formation was then measured with a 405-nm filter in an ELX800 multiwell plate reader (BioTek Instruments, USA).

UV-Visible Absorption Spectroscopy

Mixture of IgG (1.5 μM) and MG (50 μM) was prepared with or without various concentrations of ZnONPs (25, 50, and 100 μg/ml) in 0.05 M phosphate buffered saline (PBS, pH 7.4), and then incubated at 37 °C for 6 days. UV-visible absorption spectral profiles of all samples were recorded by a Cary Win UV-Vis spectrophotometer (Varian Inc., USA) in the range of 240–400 nm using quartz cuvette of 1 cm path length. Hyperchromicity at 280 nm was calculated by the following equation [6]:

$$\% \text{hyperchromicity} = \frac{\text{OD}_{\text{glycated IgG}} - \text{OD}_{\text{native IgG}}}{\text{OD}_{\text{glycated IgG}}} \times 100 \quad (2)$$

Fluorescence Spectroscopy

Mixture of IgG (1.5 μM) and MG (50 μM) was prepared with or without various concentrations of ZnONPs (25, 50, and 100 μg/ml) in 0.05 M phosphate buffered saline (PBS, pH 7.4), and then incubated at 37 °C for 6 days. Fluorescence spectra of all samples were obtained on a Jasco FP-6500 spectrofluorometer (Japan). Tryptophan fluorescence was screened on 295-nm excitation wavelengths and emission spectra were recorded in the range of 290–400 nm. Decrease in the fluorescence intensity (FI) was calculated using the following equation:

$$\% \text{decrease in FI} = \frac{F_{\text{native IgG}} - F_{\text{glycated IgG}}}{F_{\text{native IgG}}} \times 100 \quad (3)$$

The unreacted tryptophan (Try) residue percentage was calculated by considering the MG-glycated sample as a positive control, by using the following formula:

$$\% \text{untreated Try} = \left[1 - \frac{\text{Fluorescence of test group}}{\text{Fluorescence of control group}} \right] \times 100 \quad (4)$$

AGE-specific fluorescence was recorded in the emission range of 400–600 nm by exciting the samples at 370 nm [6]. Samples were put in a quartz cuvette with a 1-cm path length. Increase in fluorescence intensity was calculated using the following equation:

$$\% \text{increase in FI} = \frac{F_{\text{glycated IgG}} - F_{\text{native IgG}}}{F_{\text{glycated IgG}}} \times 100 \quad (5)$$

The percent inhibition of AGE formation was calculated by considering the MG-glycated sample as a positive control, by using the following formula:

$$\% \text{AGEs} = \left[1 - \frac{\text{Fluorescence of test group}}{\text{Fluorescence of control group}} \right] \times 100 \quad (6)$$

High-Performance Liquid Chromatography

Mixture of IgG (1.5 μM) and MG (50 μM) was prepared with or without various concentrations of ZnONPs (25, 50, and 100 μg/ml) in 0.05 M phosphate buffered saline (PBS, pH 7.4), and then incubated at 37 °C for 6 days. High-performance liquid chromatography (HPLC) was employed to CML from acid-hydrolyzed native and glycated IgG with or without ZnONP samples. The retention time of standard CML was used as reference for comparison. Briefly, hydrolyzed samples (HCL for 24 h at 110 °C) were filtrated through a 0.42-μM Millex filter. Ion-exchange HPLC column (2622 SC, 4.6 × 60 mm; Hitachi) was used to detect CML from the

filtered samples as explained earlier [42]. The accuracy and reproducibility of the HPLC method were established by repeated testing.

Circular Dichroism

Mixture of IgG (1.5 μM) and MG (50 μM) was prepared with or without various concentrations of ZnONPs (25, 50, and 100 $\mu\text{g/ml}$) in 0.05 M phosphate buffered saline (PBS, pH 7.4), and then incubated at 37 $^{\circ}\text{C}$ for 6 days. A Jasco spectropolarimeter (J-815, Japan) attached to a Jasco Peltier-type temperature controller (PTC-424S/15) was used to record far-UV circular dichroism (CD) profiles of samples. The instrument was calibrated with D-10-camphorsulphonic acid and measurements were taken at 25 $^{\circ}\text{C}$ using a temperature-controlled cell holder attached to a Neslab's RTE water bath with a temperature accuracy of ± 0.1 $^{\circ}\text{C}$. Solutions of control and glycated samples with or without ZnONPs (20 μM) were put in a 1-mm path length cuvette and spectral profiles were monitored in the range of 200–250 nm. A scan speed of 100 nm/min and response time of 1 s were selected to record the CD spectra. Three sets of each sample were studied under identical conditions to validate the reproducibility of the results [14].

Statistical Analysis

Data were examined by analysis of variance, followed by Dunnett's post hoc test for comparisons and Tukey's post hoc test for multiple comparisons. Data are presented as mean \pm SD. A statistically significant difference was defined at $p < 0.05$.

Results and Discussion

As depicted in Fig. 1, the UV–Vis spectrum of green synthesized ZnONPs in an aqueous suspension shows a characteristic single peak of ZnONPs at 370 nm (Fig. 1b), whereas no absorption peaks of plant extract were observed (Fig. 1a). Ali et al. [43] have reported the absorption peak of ZnONPs in the range of 372–375, due to surface plasmon resonance.

The crystal structure of green synthesized ZnONPs was characterized by XRD (Fig. 2). The XRD data suggested the presence of 11 distinct Bragg reflection peaks at 2θ , viz., 31.07 $^{\circ}$, 34.42 $^{\circ}$, 35.80 $^{\circ}$, 47.36 $^{\circ}$, 56.12 $^{\circ}$, 62.32 $^{\circ}$, 65.64 $^{\circ}$, 68.10 $^{\circ}$, 69.12 $^{\circ}$, 72.52 $^{\circ}$, and 76.57 $^{\circ}$ which correspond to the crystal planes (002, 004, 100–103, 110, 112, 200–202) (Fig. 2) that are in good agreement with hexagonal phase of ZnO (JCPDS CARD NO: 076-0704). The ZnONPs have an average particle size of about 42.8 nm, under our experimental conditions as calculated by using the Scherrer equation.

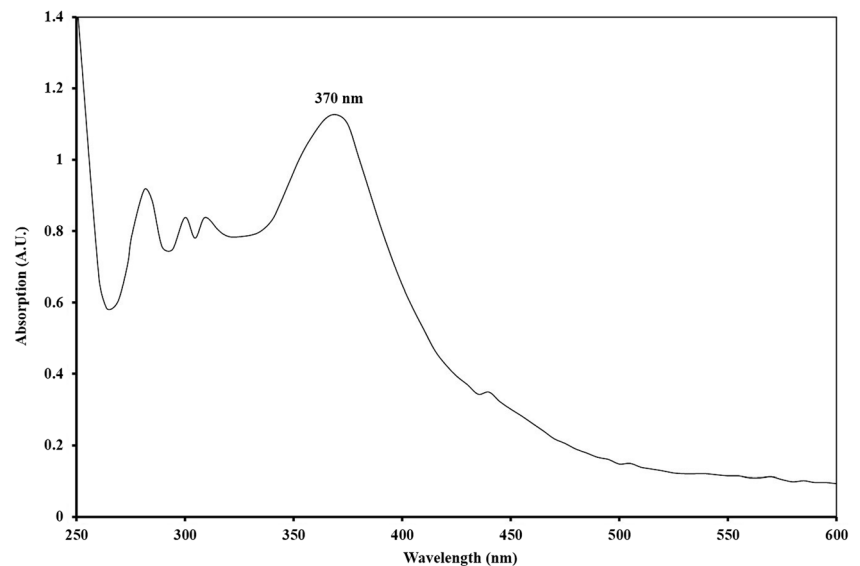
Further, the size and shape of green synthesized ZnONPs were confirmed by electron microscopy (Fig. 3a, b). Figure 3a shows that ZnONPs adopt different structures including hexagonal, spherical, and oval nanoparticles. The histogram of particle size distribution of the ZnONPs as shown in Fig. 3b revealed a normal distribution centered at 40–55 nm. The size range determined by TEM is in accordance with the data obtained in XRD. The elemental analysis of ZnONPs was done by EDX and it has been found that EDX spectrum has three emission peaks of metallic zinc (72.94%) and a single peak of oxygen (27.06%) that proves that the synthesized ZnONPs were free from impurities (Fig. 3c).

Until today, it is well established that blood proteins including IgG are glycated in AD patients by a variety of reducing sugars and metabolites, manifesting into AGE formation leading to the distortion of both structure and function of proteins [44]. Observing the generation of AGEs and oxidative stress in numbers of diseases, it is necessary to scrutinize the new molecules/compounds that could be used for the inhibition or slowing down of AGE formation. Therefore, unearthing and exploitation of nanosized molecules having clinical significance may be utilized to improve health care.

It is well known that lysine and arginine residues are highly prone to be glycated. Fluorescamine and 9,10-phenanthrenequinone assay was employed to investigate the free amino groups of lysine and arginine residues respectively, in native and MG-glycated IgG. The result showed that 62.35% of lysine residue reacted in MG-glycated IgG compared to control. A gradual decline of lysine residue reactivity was recorded in MG-glycated IgG with increasing concentrations of ZnONPs. In addition, arginine residues also reacted in the similar fashion, i.e., arginine residue reactivity decreases with increasing concentrations of ZnONPs (Table 1). Both arginine and lysine residues showed almost identical reactivity in the presence and absence of *Aloe vera* leaf extract. The above results demonstrate ZnONPs are capable of preventing the initial interaction between amino acid residues and MG, i.e., inhibit the glycation reaction at the initial stage in a concentration-dependent manner. As arginine and lysine residues occur very commonly in the antigen-binding sites of IgG, so, glycation certainly compromises the structure and function of antibodies. The findings show that ZnONPs may prevent dysfunctionalities of IgG by inhibiting the glycation reaction.

It has been reported that glycation reaction is accompanied with the generation of oxidative stress in neurodegenerative diseases resulting in enhanced oxidation of biomolecules [45–47]. Protein carbonyl content is considered as biomarker of protein oxidation [40]. In the present study, carbonyl content in MG-glycated IgG mixture in the presence or absence of *Aloe vera* leaf extract was very high (28.45 ± 1.23 nM/mg protein) compared to control (5.17 ± 1.3 nM/mg protein).

Fig. 1 UV–visible absorption spectrum of ZnONPs synthesized from *Aloe vera* leaf extract



High level of carbonyl content was observed due to oxidative modification of arginine, lysine, proline, histidine, and other amino acid residues consequential of MG-mediated glycation reaction [48]. The decrease in carbonyl content level in the reaction samples containing increasing concentration of ZnONPs (25, 50, and 100 $\mu\text{g}/\text{ml}$) was recorded (Table 1). The decreasing carbonyl content in the presence of ZnONPs is indicative of diminishing oxidation of IgG protein as a consequence of inhibitory effect of ZnONPs on glycation reaction. Previous study has proved that the presence of carbonyl contents in vivo and in vitro results from oxidative stress and predicts irreversible oxidative modifications in proteins during the glycation process [49]. In furtherance, oxidative modification induced by glycation in IgG was investigated by the evaluation of free sulfhydryl group content in protein samples by Ellman's method. The average free sulfhydryl group content of three independent assays of native IgG was 1.24 ± 0.05 nM/ml of protein. A significant decrease in free sulfhydryl group

content in MG-glycated IgG mixture with or without *Aloe vera* leaf extract was observed (0.36 ± 0.06 nM/ml) [27]. Whereas, gradual increment of free sulfhydryl group content was observed with increasing concentration of ZnONPs (Table 1). Glycation appeared to be able to affect the protein redox equilibrium towards oxidation, but ZnONPs show opposing effect on the oxidation of protein in a concentration-dependent manner. Previous studies have showed a number of AGEs and their structures in vivo and in vitro and CML and pentosidine have been reported as prominent AGEs formed during glycation [28, 50]. The CML content in native and MG-glycated IgG protein was estimated by ELISA. Significantly high levels of CML content were detected in MG-glycated IgG mixture with or without *Aloe vera* leaf extract (1.32 ± 0.51 and 1.27 ± 0.39 nM/ml IgG, respectively). In native IgG, no CML was observed; however, the MG-IgG mixture showed 1.06 ± 0.41 , 0.85 ± 0.19 , and 0.47 ± 0.26 nM/ml IgG CML content upon incubation with increasing concentrations of 25, 50, and 100 $\mu\text{g}/\text{ml}$ mM ZnONPs, respectively (Table 1). Above results indicate ZnONPs have significant strength of halting the initial stage of glycation reaction consequently decreasing the formation of CML (AGEs).

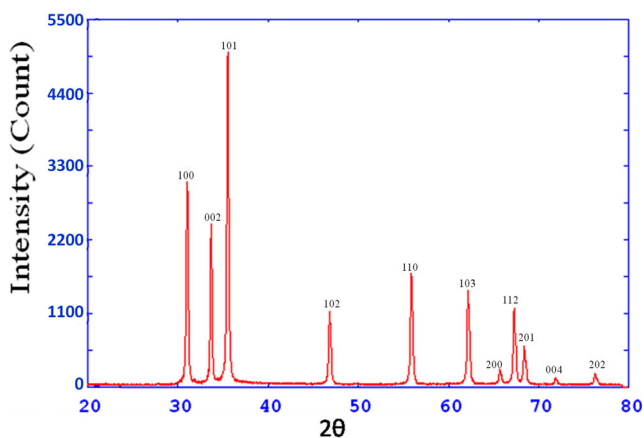


Fig. 2 X-ray diffraction patterns of ZnONPs synthesized from *Aloe vera* leaf extract

The maximum absorbance of native IgG was recorded at 280 nm on a UV–visible spectrophotometer (Fig. 4). After glycation with MG, a significant augmentation in absorbance (hyperchromicity) was recorded at 280 nm. Around 77.12% of increase of hyperchromicity was observed in the MG-glycated IgG mixture with or without *Aloe vera* leaf extract compared to native IgG at 280 nm; moreover, a remarkable increase in the absorbance between 300 and 400 nm was also observed. Whereas, when the MG-IgG mixture was incubated with increasing concentration (25, 50, and 100 $\mu\text{g}/\text{ml}$) of ZnONPs, the hyperchromicity was recorded as 62.37, 38.18, and 27.93%, respectively, compared to control as well as a

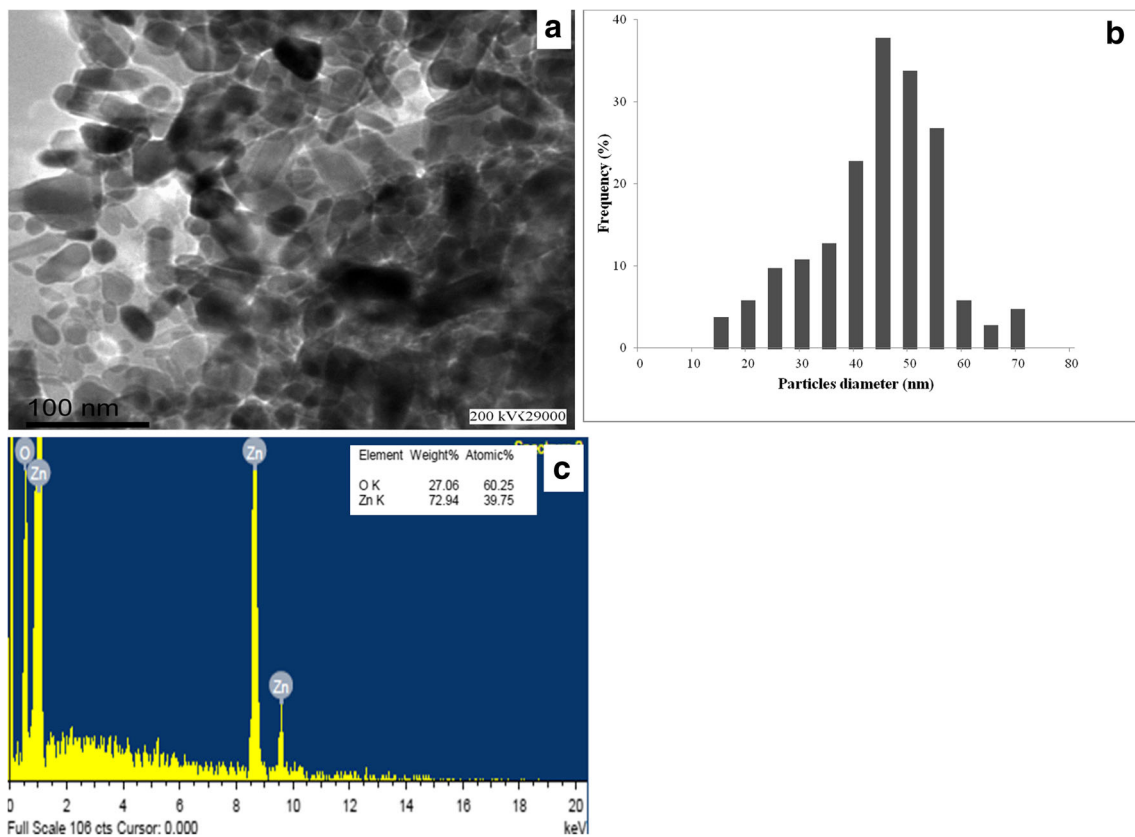


Fig. 3 HR-TEM image (a) particle size distribution histogram (b) and EDX (c) spectrum of the synthesized ZnONPs

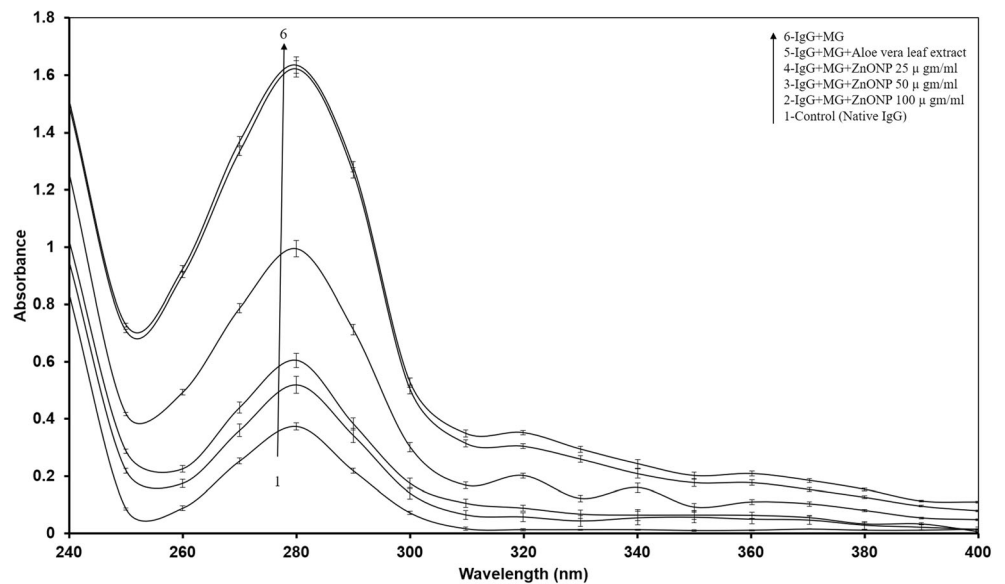
drastic decrease in absorbance between 300 and 400 nm was also observed. No significant difference in absorbance at 200–400 nm was observed in *Aloe vera* leaf extract (data not shown). The hyperchromicity in glycated IgG is due to exposure of aromatic amino acids resulting from unfolding or fragmentation of protein helix or formation of new chromophoric groups upon MG-mediated glycation. Earlier study substantiates our finding that hyperchromicity of protein is a consequence of glycation [51], as well as augmentation in absorbance from 300 to 400 nm is indicative of AGE generation [49, 51]. Additionally, an increase in absorbance between 300 and 400 nm has been found to be the reason behind proteins-AGEs/DNA-AGE formation [51].

To investigate the role of ZnONPs in AGE inhibition, fluorescent spectroscopic analysis of native and MG-glycated IgG mixtures with or without varying concentrations of ZnONPs was carried out. The samples were excited at λ_{ex} 370 nm, and the maximum emission spectral profiles were recorded at λ_{em} = 438 nm. MG-glycated IgG mixtures with or without *Aloe vera* leaf extract demonstrated more or less the same significantly high emission fluorescence intensity (87.82%) at λ_{max} 438 nm compared to native IgG. The MG-glycated IgG mixtures showed 83.67, 72.72, and 61.98% fluorescence intensity compared to native IgG, when the mixtures were incubated with increasing concentration (25, 50, and 100 μ g/ml) of ZnONPs (Fig. 5). Furthermore, 25.52, 55.40,

Table 1 Characterization of various parameters in the presence/absence of ZnONPs during glycation reaction

Sample	Lysine reacted (%)	Arginine reacted (%)	Carbonyl nM/mg protein	Free sulfhydryl group content (nM/ml protein)	CML nM/ml protein
Native IgG (control)	–	–	5.17 \pm 1.3	1.24 \pm 0.05	0
IgG + MG	62.35	56.63	28.45 \pm 1.23	0.36 \pm 0.06	1.32 \pm 0.51
IgG + MG + <i>Aloe vera</i> Leaf extract	60.75	51.23	26.15 \pm 1.18	0.29 \pm 0.08	1.27 \pm 0.39
IgG + MG + AgNP 0.09 mM	48.44	45.72	23.05 \pm 1.11	0.52 \pm 0.07	1.06 \pm 0.41
IgG + MG + AgNP 0.18 mM	39.67	37.11	19.50 \pm 1.13	0.73 \pm 0.09	0.85 \pm 0.19
IgG + MG + AgNP 0.27 mM	21.69	20.75	9.60 \pm 1.05	0.93 \pm 0.12	0.47 \pm 0.26

Fig. 4 UV absorbance spectra of IgG and MG with different concentrations of ZnONPs incubated at 37 °C for 6 days. UV absorbance was screened at 280 nm

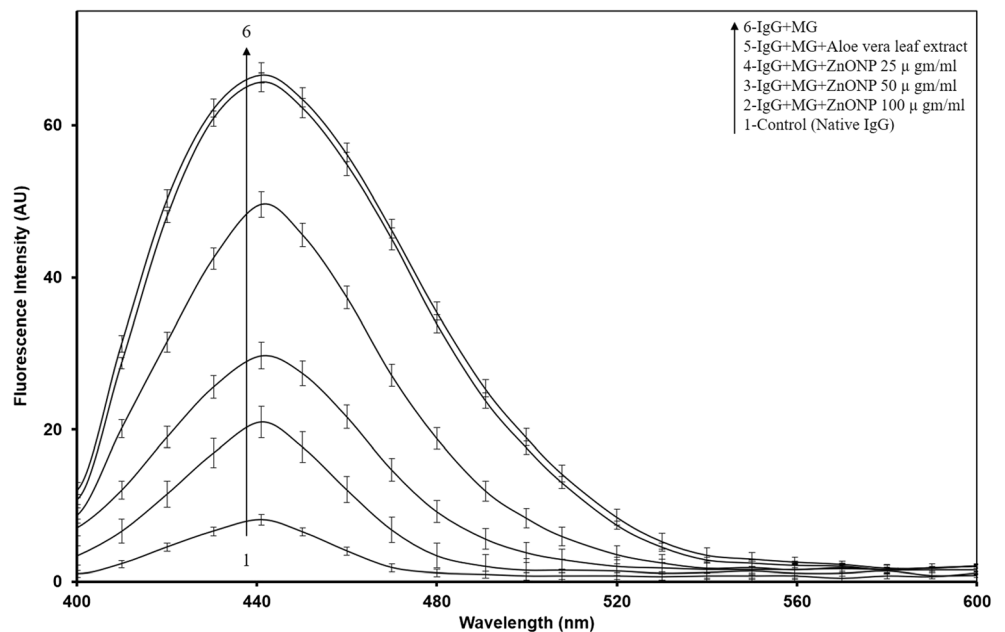


and 68.01% inhibition of AGE formation was observed at 25, 50, and 100 µg/ml ZnONPs respectively, compared to MG-IgG mixture with or without *Aloe vera* leaf extract (Fig. 4). Our outcomes are steady with previous studies as a number of AGEs exhibit a characteristic fluorescence at about 370/438 nm and fluorescence intensity is employed to examine the formation of AGEs under various treatments [52, 53]. The results clearly indicate that ZnONPs inhibited the AGE formation on a concentration-dependent manner.

Formation and inhibition of AGEs in glycation system in the presence or absence of ZnONPs were again investigated by HPLC. The acid-hydrolyzed samples were subjected to HPLC. The HPLC profile of standard CML was taken as reference to verify formation of CML in native and MG-

glycated IgG with or without ZnONP samples. Standard CML exhibited a well-defined and clear peak at the retention of 24.80 min (Fig. 6a). The chromatogram of native IgG (Fig. 6b) showed no remarkable peak analogous to standard CML. The chromatogram of MG-glycated IgG sample exhibited a corresponding prominent peak with a retention time of 25.55 min (Fig. 6c). The peak observed in MG-glycated IgG sample is almost analogous to the standard CML, but MG-glycated IgG sample in the presence of ZnONPs showed peaks more or less at the same retention time to that of standard CML, but peak height gradually decreased with increasing concentration of ZnONPs (Fig. 6d–f). The above findings substantiate to each other that ZnONPs have tremendous inhibitory effect on AGE formation in a concentration-

Fig. 5 Fluorescence emission intensity profiles of IgG and MG with different concentrations of ZnONPs. Fluorescence intensities were recorded at excitation and emission wavelengths of 370 and 438 nm, respectively



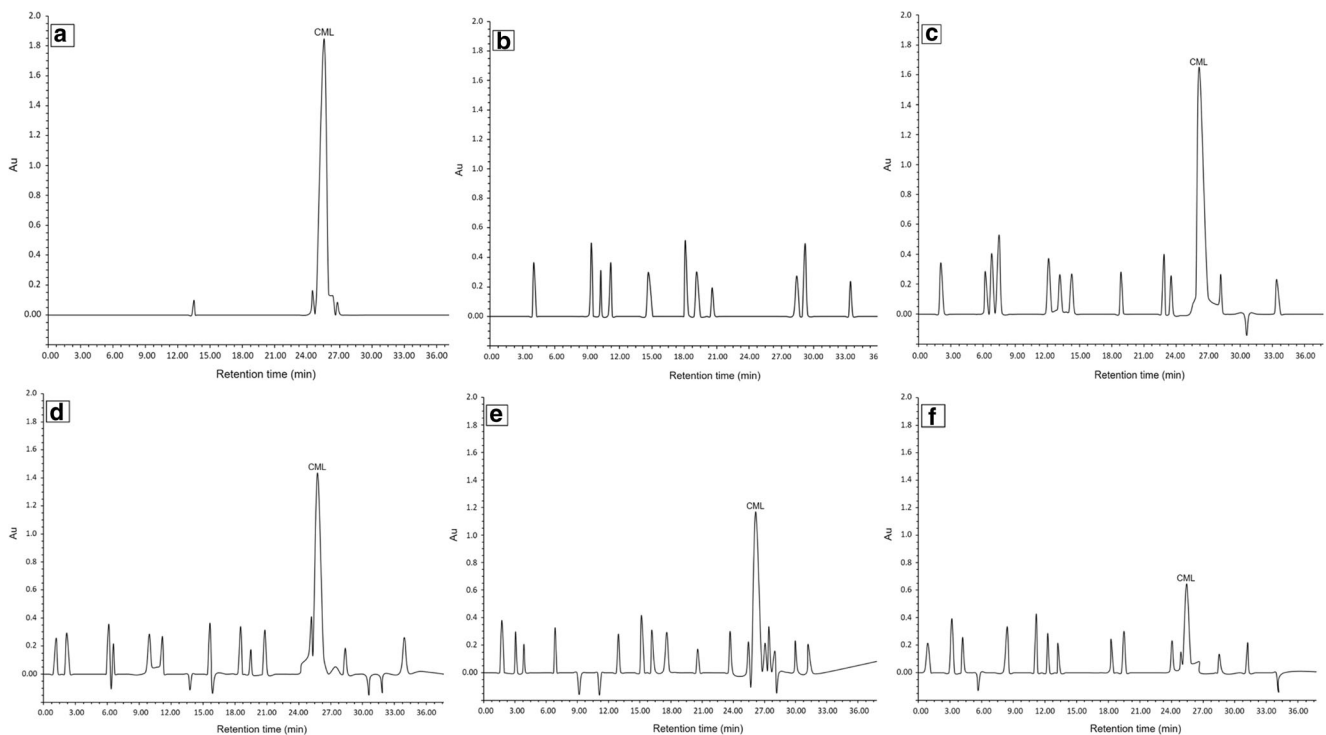


Fig. 6 HPLC chromatogram of IgG with MG mixtures with or without ZnONPs after 6 days of incubation. HPLC profiles of **a** standard CML, **b** native IgG, **c** IgG–MG mixtures without ZnONPs, **d** IgG–MG with

ZnONPs (25 $\mu\text{g/ml}$), **e** HSA–MG with ZnONPs (50 $\mu\text{g/ml}$), and **f** IgG–MG with ZnONPs (100 $\mu\text{g/ml}$)

dependent manner. Hence, our study reports go parallel with previous findings that showed various nanoparticles (selenium, gold, and silver) were AGE inhibitor [54–56].

The intrinsic fluorescence of tryptophan residues in human IgG was exploited to obtain information on damage or change in the microenvironment of these residues resulting from glycation. Native and MG-glycated IgG with or without ZnONP samples were excited at 285 nm and emission

intensity was recorded at 335 nm (Fig. 7). Compared to native IgG, a noticeable decrease in emission intensity of MG-glycated IgG with or without *Aloe vera* leaf extract was observed (79.61%). Whereas, MG-glycated IgG mixture with increasing concentration of ZnONP gradual decrease in emission intensity was observed (66.33, 39.20, and 21.13%). Decrease of the tryptophan fluorescence in MG-glycated IgG is attributed to the damage of tryptophan and/or modification

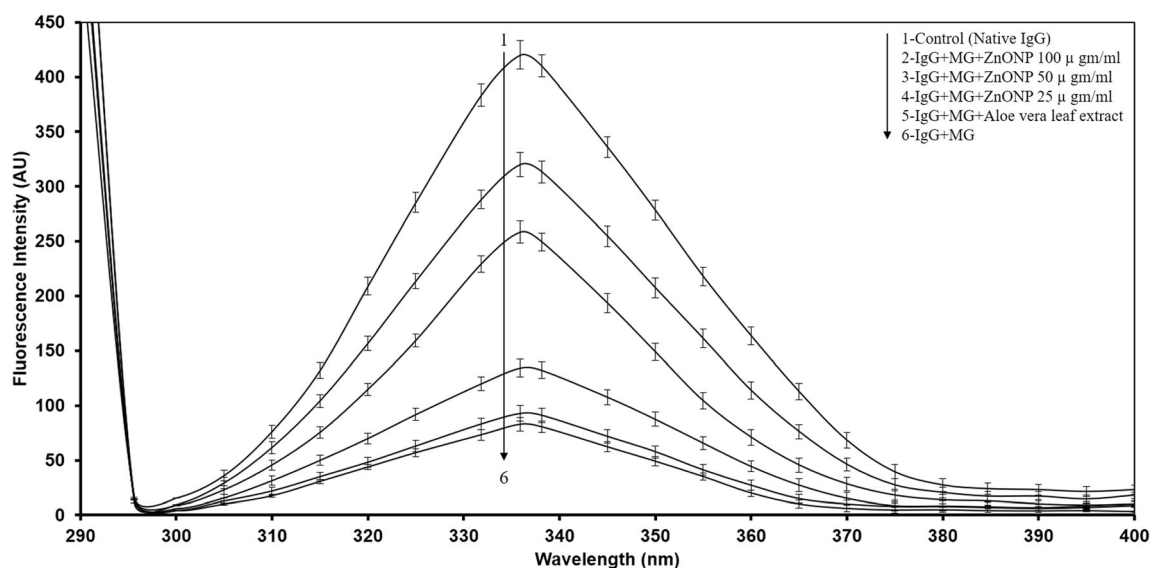


Fig. 7 Fluorescence emission profile of native IgG and MG with different concentrations of ZnONPs. Fluorescence intensities were recorded at excitation and emission wavelengths of 295 and 335 nm, respectively

of tryptophan microenvironment upon MG-mediated glycation (30, sanam). Moreover, 39.57, 67.0, and 74.13% tryptophan residues did not react or were not damaged by MG in the presence of increasing concentration of ZnONPs. Damage of tryptophan affects the whole structure of the protein [57, 58]. Increase in fluorescence intensity in the presence of ZnONPs indicates that ZnONPs resist the damage of IgG and protect the structure of IgG.

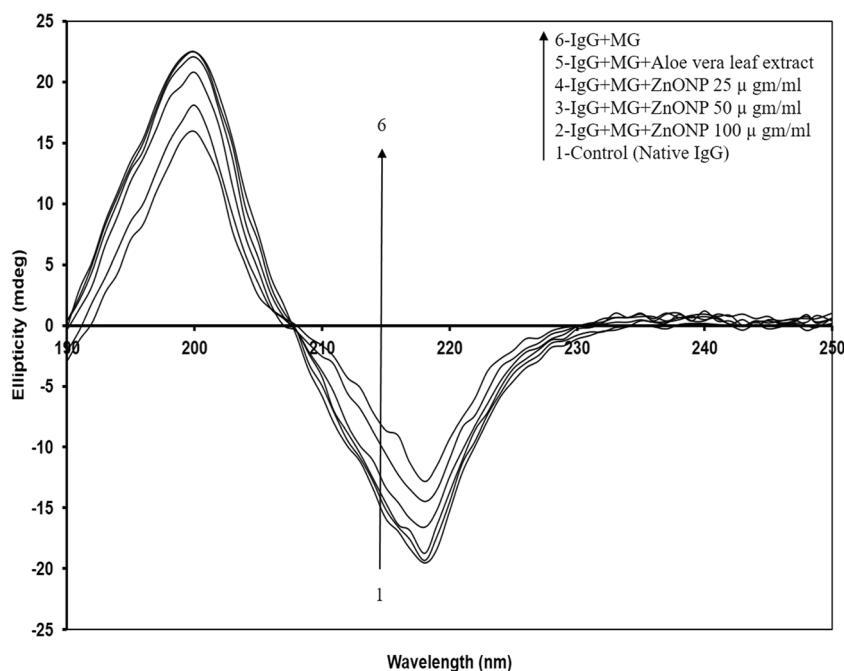
Far-UV CD spectroscopy is specifically employed to examine the secondary structure and conformational changes in proteins [59, 60]. The samples were subjected to ellipticity [θ] investigations in far-UV region (190–250 nm). Native IgG displayed typical CD spectrum of a β -sheeted protein with negative minima at 217 nm, positive maxima at 200 nm, and zero ellipticity at 208 nm (Fig. 8) [61]. CD spectra of MG-glycated IgG demonstrated increased ellipticity at 217 nm and decreased ellipticity at 200 nm, compared to native IgG. The findings indicate that MG-mediated glycation has caused substantial loss of β structure and increase in α -helix structure of IgG. Previous studies have reported a loss of secondary structure due to unfolding of IgG [2] which confirms our findings. When the MG–IgG mixture was incubated with increasing concentration of ZnONPs, an opposite trend in ellipticity change was observed at 217 and 200 nm. CD and fluorescence study clearly showed that ZnONPs oppose the change in secondary structure of IgG in a concentration-dependent manner. Overall, this study shows that ZnONPs act as a very potent anti-glycating agent inhibiting the formation of AGEs as well as ZnONPs resist the structural change in protein and maintain secondary structure of protein. Previous studies have reported the anti-glycating and anti-oxidative activities of nanoparticles

that comprehensively reduce glycation reactions consequently affecting the AGE formation [6, 62]. Likewise, our recent studies have shown that silver nanoparticles are very potent anti-glycating agents and protect protein from denaturation as well [6, 63].

Accumulating evidences suggest AGEs play a significant role in the pathogenesis of neurodegenerative disorders including Parkinson's and Alzheimer's disease, as well as diabetic neuropathy, a diabetes-associated complication [1, 5, 64]. Indeed, *in vivo* inhibition of AGE generation is accompanied with decrease in the severity of disease and its progression [65, 66]. Similarly, the evidence provided in the study, i.e., ZnONP-mediated inhibition of glycation as well as prevention of structural modification of proteins, may be exploited against AGE and AGE-mediated damage in neurodegenerative disorders. In addition, recently, therapeutic potential of ZnONP is presented in several studies in various peripheral disease experimental models including *ex vivo* [67] and *in vivo* [68] with promising outcome. Therefore, therapeutic potential of ZnONP may be utilized in the delay of disease progression and/or reversal of disease pathogenesis in AGE-related neurodegenerative disorders; however, further elucidation is required to ascertain its efficacy in the prevention of AGE generation in *in vivo* model.

Interaction of nanoparticles with proteins is the basis of nanoparticle bio-reactivity. Our knowledge about the biocompatibility and risks of exposure to nanomaterials is limited. In a biological medium, NPs may interact with biomolecules such as proteins, nucleic acids, lipids, and even biological metabolites due to their nanosize and large surface-to-mass ratio [69, 70]. Binding of proteins at the nano–bio interface

Fig. 8 CD profiles of IgG–MG with and without various concentrations of ZnONPs incubated at 37 °C for 6 days. All samples were appropriately diluted with deionized water before recording the CD profiles. Repeat studies revealed no significant difference in CD profiles



is aided by several forces such as hydrogen bonds, solvation forces, and Van der Waals interactions. The overall NP–PC formation is a multifactorial process and depends not only on the characteristics of the nanoparticles but also on the chemical properties of individual proteins and their structural flexibility also plays an important role in regulating such surface-driven modifications to their secondary structures [71, 72]. There are conflicting reports on the structural change of protein interaction with nanoparticles. Many studies have shown that when bovine serum albumin (BSA) protein interacted with carbon C60 fullerene and ZnO nanoparticles, no major conformational change was recorded [73–75]. Furthermore, the structure and thermodynamic stability of cytochrome c was not significantly affected by its interaction with ZnO nanoparticles [76]. However, Turci et al. showed that RNase and lysozyme retained their native structures on silica NP while albumin and lactoperoxidase underwent an irreversible conformational change [77]. In addition, gold NPs were shown to influence conformational changes in the structure of BSA in a dose-dependent manner [78]. The reports show that different proteins and nanoparticles affect the protein structure differently. Further in vivo as well as in vitro studies are essentially required to understand the effects of nanoparticle–protein interaction on biokinetics, absorption, tissue distribution, bioavailability, and potential toxicity. Also, it is important to mention that Maillard reaction might be influenced by several factors such as temperature, pH, concentration and type of reducing sugar, concentration and types of amino acids, chemical compounds, or inhibitors, and water content [79–81]. Several in vitro studies of various reducing sugars and amino acid glycation systems have showed that the glycation reaction (Maillard reaction) is pH dependent, where it was observed that at low pH or acidic conditions, no glycation reaction was observed, while at increased pH or alkaline conditions, glycation reaction (Maillard reaction) was found to be increased [82–84].

Nanomedicine has recently emerged as a better option for the treatment of various CNS diseases. However, the utter multiplicity of the physicochemical parameters of nanoparticles such as size, shape, structure, and elemental constituents makes the investigation of their toxic effects complex and challenging [85–87]. Nanoparticle-mediated ROS responses have been reported to orchestrate a series of pathological events such as genotoxicity, age-related inflammation, and fibrosis. Other NPs such as titanium dioxide (TiO₂), zinc oxide (ZnO), cerium oxide (CeO₂), and silver NP have been shown to deposit on the cellular surface or inside the subcellular organelles and induce oxidative stress signaling cascades that eventually result in oxidative stress to the cell [88]. The majority of in vivo toxicity studies on ZnO nanoparticles have investigated acute toxicity and subacute toxicity after a single or repeated dosing, respectively, via inhalation, ingestion, injection, or dermal penetration [89–91].

To date, there are previous reports on the cytotoxic and genotoxic effect of ZnO nanoparticles in vitro and in vivo system [92]. However, these nanotoxicology-based studies reported numerous conflicting results due to slight differences in the physicochemical features of nanoparticles used under studies [93]. Several studies have demonstrated that the differences were generated by the size and surface charge of nanoparticles [94–96]. For instance, the selenium NPs did not show cytotoxic effect on BV-2, BRL-3A, and HepG2 cells. In addition, these three kinds of cells have been employed to evaluate cytotoxicity of nanoparticles in other studies [97–99]. There were no significant changes in morphology or cell quantity in microglial BV-2 and BRL-3A cells treated with Se NPs. Although toxic effects of zinc oxide nanoparticles (ZnONPs) have been previously studied, there are still controversies in terms of dose, size, shape, and affecting cells. Therefore, findings suggest that toxicity depends on physicochemical features of nanoparticles, so cautious manipulation of this information will aid in the creation of biocompatible and clinically feasible nanoparticles and will therefore contribute to the advancement of the field of nanomedicine.

Apparently, precise and clear mechanism of ZnONP action is still unclear. However, there are few explanations about the mechanisms of nanoparticle inhibitory activity. Specifically, free amino group of amino acids, as well as N-terminal amino acids, is the key sites to be attacked by glycation agents. It is considered that anti-glycation agents competitively bind to these sites. Additionally, observations suggest that diminution/prevention of AGE formation may be a consequence of covering of amino groups or sequestration of reacting group of glycation species by ZnONPs [100]. Further investigations are required and guaranteed [101].

Conclusions

Glycation reaction starts a vicious cycle following free radicals, carbonyls species, and AGE production, playing a critical role in the initiation/propagation of several diseases specifically in neurodegenerative conditions. Considering the menacing role of AGEs, several anti-glycation agents have been discovered but the exploration of more effective agents is the need of the hour to resolve this grave clinical issue. It has been found that zinc oxide is a fairly good antioxidant and may play a vital role in AGE inhibition. In this study, biosynthesized ZnONPs have displayed strong capability of antioxidant and anti-glycation agent as well as defended protein from damage by methylglyoxal. Therefore, it may be exploited as therapeutics in the prevention or reversal of underlying pathology of CNS diseases. On the other hand, a methodical and mechanistic approach is necessary before consequential role of nanoparticles can be applied in medical field.

Acknowledgements The authors thank Jazan University, Saudi Arabia, and Institute of Research and Medical Consultations (IRMC), Imam Abdulrahman Bin Faisal University, Dammam, Saudi Arabia, for providing instruments, facilities, and other items used in this study.

References

- Gasiorowski K, Brokos B, Echeverria V, Barreto GE, Leszek J (2017) RAGE-TLR crosstalk sustains chronic inflammation in neurodegeneration. *Mol Neurobiol*. <https://doi.org/10.1007/s12035-017-0419-4>
- Arfat MY, Ashraf JM, Arif Z, Moinuddin, Alam K (2014) Fine characterization of glucosylated human IgG by biochemical and biophysical methods. *Int J Biol Macromol* 69:408–415. <https://doi.org/10.1016/j.ijbiomac.2014.05.069>
- Uribarri J, Cai W, Peppas M, Goodman S, Ferrucci L, Striker G, Vlassara H (2007) Circulating glycotoxins and dietary advanced glycation endproducts: two links to inflammatory response, oxidative stress, and aging. *J Gerontol A Biol Sci Med Sci* 62(4):427–433
- Ashraf JM, Arif B, Dixit K, Moinuddin, Alam K (2012) Physicochemical analysis of structural changes in DNA modified with glucose. *Int J Biol Macromol* 51(4):604–611. <https://doi.org/10.1016/j.ijbiomac.2012.06.013>
- Munch G, Thome J, Foley P, Schinzel R, Riederer P (1997) Advanced glycation endproducts in ageing and Alzheimer's disease. *Brain Res Brain Res Rev* 23(1–2):134–143
- Ashraf JM, Ansari MA, Khan HM, Alzohairy MA, Choi I (2016) Green synthesis of silver nanoparticles and characterization of their inhibitory effects on AGEs formation using biophysical techniques. *Sci Rep* 6(1):20414. <https://doi.org/10.1038/srep20414>
- Ashraf JM, Rabbani G, Ahmad S, Hasan Q, Khan RH, Alam K, Choi I (2015) Glycation of H1 histone by 3-deoxyglucosone: effects on protein structure and generation of different advanced glycation end products. *PLoS One* 10(6):e0130630. <https://doi.org/10.1371/journal.pone.0130630>
- Chetyrkin SV, Mathis ME, Ham AJ, Hachey DL, Hudson BG, Voziyan PA (2008) Propagation of protein glycation damage involves modification of tryptophan residues via reactive oxygen species: inhibition by pyridoxamine. *Free Radic Biol Med* 44(7):1276–1285. <https://doi.org/10.1016/j.freeradbiomed.2007.09.016>
- Thornalley PJ (1998) Glutathione-dependent detoxification of alpha-oxoaldehydes by the glyoxalase system: involvement in disease mechanisms and antiproliferative activity of glyoxalase I inhibitors. *Chem Biol Interact* 111–112:137–151. [https://doi.org/10.1016/S0009-2797\(97\)00157-9](https://doi.org/10.1016/S0009-2797(97)00157-9)
- Tajes M, Eraso-Pichot A, Rubio-Moscardo F, Guivernau B, Bosch-Morato M, Valls-Comamala V, Munoz FJ (2014) Methylglyoxal reduces mitochondrial potential and activates Bax and caspase-3 in neurons: Implications for Alzheimer's disease. *Neurosci Lett* 580:78–82. <https://doi.org/10.1016/j.neulet.2014.07.047>
- Angeloni C, Zamboni L, Hrelia S (2014) Role of methylglyoxal in Alzheimer's disease. *Biomol Res Int* 2014:238485. <https://doi.org/10.1155/2014/238485>
- Tajes M, Eraso-Pichot A, Rubio-Moscardo F, Guivernau B, Ramos-Fernandez E, Bosch-Morato M, Guix FX, Clarimon J et al (2014) Methylglyoxal produced by amyloid-beta peptide-induced nitrotyrosination of triosephosphate isomerase triggers neuronal death in Alzheimer's disease. *J Alzheimer's Dis* 41(1):273–288. <https://doi.org/10.3233/JAD-131685>
- Lo TW, Westwood ME, McLellan AC, Selwood T, Thornalley PJ (1994) Binding and modification of proteins by methylglyoxal under physiological conditions. A kinetic and mechanistic study with N alpha-acetylarginine, N alpha-acetylcysteine, and N alpha-acetylysine, and bovine serum albumin. *J Biol Chem* 269(51):32299–32305
- Rabbani G, Ahmad E, Zaidi N, Fatima S, Khan RH (2012) pH-induced molten globule state of Rhizopus niveus lipase is more resistant against thermal and chemical denaturation than its native state. *Cell Biochem Biophys* 62(3):487–499. <https://doi.org/10.1007/s12013-011-9335-9>
- Burton DR, Gregory L, Jefferis R (1986) Aspects of the molecular structure of IgG subclasses. *Monogr Allergy* 19:7–35
- Dolhofer R, Siess EA, Wieland OH (1985) Nonenzymatic glycation of immunoglobulins leads to an impairment of immunoreactivity. *Biol Chem Hoppe Seyler* 366(4):361–366. <https://doi.org/10.1515/bchm3.1985.366.1.361>
- Dolhofer-Bliesener R, Gerbitz KD (1990) Effect of nonenzymatic glycation on the structure of immunoglobulin G. *Biol Chem Hoppe Seyler* 371(8):693–697. <https://doi.org/10.1515/bchm3.1990.371.2.693>
- Kaminsky YG, Reddy VP, Ashraf GM, Ahmad A, Benberin VV, Kosenko EA, Aliev G (2013) Age-related defects in erythrocyte 2, 3-diphosphoglycerate metabolism in dementia. *Aging Dis* 4(5):244–255. <https://doi.org/10.14336/AD.2013.0400244>
- Reddy VP, Beyaz A (2006) Inhibitors of the Maillard reaction and AGE breakers as therapeutics for multiple diseases. *Drug Discov Today* 11(13–14):646–654. <https://doi.org/10.1016/j.drudis.2006.05.016>
- Li XH, Du LL, Cheng XS, Jiang X, Zhang Y, Lv BL, Liu R, Wang JZ et al (2013) Glycation exacerbates the neuronal toxicity of beta-amyloid. *Cell Death Dis* 4(6):e673. <https://doi.org/10.1038/cddis.2013.180>
- Webster J, Urban C, Berbaum K, Loske C, Alpar A, Gartner U, de Arriba SG, Arendt T et al (2005) The carbonyl scavengers aminoguanidine and nilisetam protect against the neurotoxic effects of methylglyoxal. *Neurotox Res* 7(1–2):95–101
- Jaturapatpom D, Isaac MG, McCleery J, Tabet N (2012) Aspirin, steroidal and non-steroidal anti-inflammatory drugs for the treatment of Alzheimer's disease. *Cochrane Database Syst Rev* 2:CD006378. <https://doi.org/10.1002/14651858.CD006378.pub2>
- Albarracin SL, Stab B, Casas Z, Sutachan JJ, Samudio I, Gonzalez J, Gonzalo L, Capani F et al (2012) Effects of natural antioxidants in neurodegenerative disease. *Nutr Neurosci* 15(1):1–9. <https://doi.org/10.1179/1476830511Y.0000000028>
- Sutachan JJ, Casas Z, Albarracin SL, Stab BR 2nd, Samudio I, Gonzalez J, Morales L, Barreto GE (2012) Cellular and molecular mechanisms of antioxidants in Parkinson's disease. *Nutr Neurosci* 15(3):120–126. <https://doi.org/10.1179/1476830511Y.0000000033>
- Dey A, Bhattacharya R, Mukherjee A, Pandey DK (2017) Natural products against Alzheimer's disease: pharmacotherapeutics and biotechnological interventions. *Biotechnol Adv* 35(2):178–216. <https://doi.org/10.1016/j.biotechadv.2016.12.005>
- Natarajan S, Shunmugiah KP, Kasi PD (2013) Plants traditionally used in age-related brain disorders (dementia): an ethanopharmacological survey. *Pharm Biol* 51(4):492–523. <https://doi.org/10.3109/13880209.2012.738423>
- Ahmad S, Moinuddin, Ali A (2012) Immunological studies on glycated human IgG. *Life Sci* 90(25–26):980–987. <https://doi.org/10.1016/j.lfs.2012.05.002>
- Ahmed MU, Thorpe SR, Baynes JW (1986) Identification of N epsilon-carboxymethyllysine as a degradation product of fructoselysine in glycated protein. *J Biol Chem* 261(11):4889–4894
- Leszek J, Md Ashraf G, Tse WH, Zhang J, Gasiorowski K, Avila-Rodriguez MF, Tarasov VV, Barreto GE et al (2017) Nanotechnology

- for Alzheimer disease. *Curr Alzheimer Res* 14(11):1182–1189. <https://doi.org/10.2174/1567205014666170203125008>
30. Huang B, Zhang J, Hou J, Chen C (2003) Free radical scavenging efficiency of nano-Se in vitro. *Free Radic Biol Med* 35(7):805–813. [https://doi.org/10.1016/S0891-5849\(03\)00428-3](https://doi.org/10.1016/S0891-5849(03)00428-3)
 31. Kim JH, Hong CO, Koo YC, Choi HD, Lee KW (2012) Antiglycation effect of gold nanoparticles on collagen. *Biol Pharm Bull* 35(2):260–264. <https://doi.org/10.1248/bpb.35.260>
 32. Mazo NA, Echeverria V, Cabezas R, Avila-Rodriguez M, Aliev G, Leszek J, Barreto GE (2017) Medicinal plants as protective strategies against Parkinson's disease. *Curr Pharm Des* 23(28):4180–4188. <https://doi.org/10.2174/1381612823666170316142803>
 33. Singh SK, Barreto GE, Aliev G, Echeverria V (2017) Ginkgo biloba as an alternative medicine in the treatment of anxiety in dementia and other psychiatric disorders. *Curr Drug Metab* 18(2):112–119. <https://doi.org/10.2174/1389200217666161201112206>
 34. Leszek J, Barreto GE, Gasiorowski K, Koutsouraki E, Avila-Rodrigues M, Aliev G (2016) Inflammatory mechanisms and oxidative stress as key factors responsible for progression of neurodegeneration: role of brain innate immune system. *CNS Neurol Disord Drug Targets* 15(3):329–336. <https://doi.org/10.2174/1871527315666160202125914>
 35. Cabezas R, El-Bacha RS, Gonzalez J, Barreto GE (2012) Mitochondrial functions in astrocytes: neuroprotective implications from oxidative damage by rotenone. *Neurosci Res* 74(2):80–90. <https://doi.org/10.1016/j.neures.2012.07.008>
 36. Seneviratne C, Dombi GW, Liu W, Dain JA (2011) The in vitro glycation of human serum albumin in the presence of Zn(II). *J Inorg Biochem* 105(12):1548–1554. <https://doi.org/10.1016/j.jinorgbio.2011.09.001>
 37. Ansari MA, Khan HM, Khan AA, Sultan A, Azam A (2012) Synthesis and characterization of the antibacterial potential of ZnO nanoparticles against extended-spectrum beta-lactamases-producing *Escherichia coli* and *Klebsiella pneumoniae* isolated from a tertiary care hospital of North India. *Appl Microbiol Biotechnol* 94(2):467–477. <https://doi.org/10.1007/s00253-011-3733-1>
 38. Udenfriend S, Stein S, Bohlen P, Dairman W, Leimgruber W, Weigele M (1972) Fluorescamine: a reagent for assay of amino acids, peptides, proteins, and primary amines in the picomole range. *Science* 178(4063):871–872. <https://doi.org/10.1126/science.178.4063.871>
 39. Smith RE, MacQuarrie R (1978) A sensitive fluorometric method for the determination of arginine using 9,10-phenanthrenequinone. *Anal Biochem* 90(1):246–255. [https://doi.org/10.1016/0003-2697\(78\)90029-5](https://doi.org/10.1016/0003-2697(78)90029-5)
 40. Levine RL, Williams JA, Stadtman ER, Shacter E (1994) Carbonyl assays for determination of oxidatively modified proteins. *Methods Enzymol* 233:346–357. [https://doi.org/10.1016/S0076-6879\(94\)33040-9](https://doi.org/10.1016/S0076-6879(94)33040-9)
 41. Sedlak J, Lindsay RH (1968) Estimation of total, protein-bound, and nonprotein sulfhydryl groups in tissue with Ellman's reagent. *Anal Biochem* 25(1):192–205. [https://doi.org/10.1016/0003-2697\(68\)90092-4](https://doi.org/10.1016/0003-2697(68)90092-4)
 42. Ikeda K, Higashi T, Sano H, Jinnouchi Y, Yoshida M, Araki T, Ueda S, Horiuchi S (1996) N (epsilon)-(carboxymethyl)lysine protein adduct is a major immunological epitope in proteins modified with advanced glycation end products of the Maillard reaction. *Biochemistry* 35(24):8075–8083. <https://doi.org/10.1021/bi9530550>
 43. Ali K, Dwivedi S, Azam A, Saquib Q, Al-Said MS, Alkhedhairi AA, Musarrat J (2016) Aloe vera extract functionalized zinc oxide nanoparticles as nanoantibiotics against multi-drug resistant clinical bacterial isolates. *J Colloid Interface Sci* 472:145–156. <https://doi.org/10.1016/j.jcis.2016.03.021>
 44. Loeffler DA (2014) Should development of Alzheimer's disease-specific intravenous immunoglobulin be considered? *J Neuroinflammation* 11(1):198. <https://doi.org/10.1186/s12974-014-0198-z>
 45. Khan TA, Hassan I, Ahmad A, Perveen A, Aman S, Quddusi S, Alhazza IM, Ashraf GM et al (2016) Recent updates on the dynamic association between oxidative stress and neurodegenerative disorders. *CNS Neurol Disord Drug Targets* 15(3):310–320. <https://doi.org/10.2174/1871527315666160202124518>
 46. Aliev G, Priyadarshini M, Reddy VP, Grieg NH, Kaminsky Y, Cacabelos R, Ashraf GM, Jabir NR et al (2014) Oxidative stress mediated mitochondrial and vascular lesions as markers in the pathogenesis of Alzheimer disease. *Curr Med Chem* 21(19):2208–2217. <https://doi.org/10.2174/0929867321666131227161303>
 47. Abate G, Marziano M, Rungratanawanich W, Memo M, Uberti D (2017) Nutrition and AGE-ing: focusing on Alzheimer's disease. *Oxidative Med Cell Longev* 2017:7039816–7039810. <https://doi.org/10.1155/2017/7039816>
 48. Dalle-Donne I, Rossi R, Giustarini D, Milzani A, Colombo R (2003) Protein carbonyl groups as biomarkers of oxidative stress. *Clin Chim Acta; Int J Clin Chem* 329(1–2):23–38
 49. Schmitt A, Gasic-Milenkovic J, Schmitt J (2005) Characterization of advanced glycation end products: mass changes in correlation to side chain modifications. *Anal Biochem* 346(1):101–106. <https://doi.org/10.1016/j.ab.2005.07.035>
 50. Wells-Knecht KJ, Brinkmann E, Wells-Knecht MC, Litchfield JE, Ahmed MU, Reddy S, Zyzak DV, Thorpe SR et al (1996) New biomarkers of Maillard reaction damage to proteins. *Nephrol Dial Transplant* 11(Suppl 5):41–47
 51. Kessel L, Kalinin S, Nagaraj RH, Larsen M, Johansson LB (2002) Time-resolved and steady-state fluorescence spectroscopic studies of the human lens with comparison to argpyrimidine, pentosidine and 3-OH-kynurenine. *Photochem Photobiol* 76(5):549–554
 52. Liggins J, Furth AJ (1997) Role of protein-bound carbonyl groups in the formation of advanced glycation endproducts. *Biochim Biophys Acta* 1361(2):123–130. [https://doi.org/10.1016/S0925-4439\(97\)00023-9](https://doi.org/10.1016/S0925-4439(97)00023-9)
 53. Obayashi H, Nakano K, Shigeta H, Yamaguchi M, Yoshimori K, Fukui M, Fujii M, Kitagawa Y et al (1996) Formation of crossline as a fluorescent advanced glycation end product in vitro and in vivo. *Biochem Biophys Res Commun* 226(1):37–41. <https://doi.org/10.1006/bbrc.1996.1308>
 54. Bhattacharya J, Jasarapuria S, Sarkar T, GhoshMoulick R, Dasgupta AK (2007) Gold nanoparticle-based tool to study protein conformational variants: implications in hemoglobinopathy. *Nanomed: Nanotechnol Biol Med* 3(1):14–19. <https://doi.org/10.1016/j.nano.2006.10.159>
 55. Singha S, Bhattacharya J, Datta H, Dasgupta AK (2009) Antiglycation activity of gold nanoparticles. *Nanomed: Nanotechnol Biol Med* 5(1):21–29. <https://doi.org/10.1016/j.nano.2008.06.005>
 56. Yu S, Zhang W, Liu W, Zhu W, Guo R, Wang Y, Zhang D, Wang J (2015) The inhibitory effect of selenium nanoparticles on protein glycation in vitro. *Nanotechnology* 26(14):145703. <https://doi.org/10.1088/0957-4484/26/14/145703>
 57. Davies KJ, Delsignore ME, Lin SW (1987) Protein damage and degradation by oxygen radicals. II Modification of amino acids. *J Biol Chem* 262(20):9902–9907
 58. Shaklai N, Garlick RL, Bunn HF (1984) Nonenzymatic glycosylation of human serum albumin alters its conformation and function. *J Biol Chem* 259(6):3812–3817
 59. Ashraf GM, Rizvi S, Naqvi S, Suhail N, Bilal N, Hasan S, Tabish M, Banu N (2010) Purification, characterization, structural analysis and protein chemistry of a buffalo heart galectin-1. *Amino Acids* 39(5):1321–1332. <https://doi.org/10.1007/s00726-010-0574-7>

60. Ashraf GM, Banu N, Ahmad A, Singh LP, Kumar R (2011) Purification, characterization, sequencing and biological chemistry of galectin-1 purified from *Capra hircus* (goat) heart. *Protein J* 30(1):39–51. <https://doi.org/10.1007/s10930-010-9300-2>
61. Hawe A, Kasper JC, Friess W, Jiskoot W (2009) Structural properties of monoclonal antibody aggregates induced by freeze-thawing and thermal stress. *Eur J Pharm Sci* 38(2):79–87. <https://doi.org/10.1016/j.ejps.2009.06.001>
62. Ashe S, Nayak D, Kumari M, Nayak B (2016) Ameliorating effects of green synthesized silver nanoparticles on glycated end product induced reactive oxygen species production and cellular toxicity in osteogenic Saos-2 cells. *ACS Appl Mater Interfaces* 8(44):30005–30016. <https://doi.org/10.1021/acsami.6b10639>
63. Ashraf JM, Ansari MA, Choi I, Khan HM, Alzohairy MA (2014) Antilycating potential of gum arabic capped-silver nanoparticles. *Appl Biochem Biotechnol* 174(1):398–410. <https://doi.org/10.1007/s12010-014-1065-1>
64. Thornalley PJ (2002) Glycation in diabetic neuropathy: characteristics, consequences, causes, and therapeutic options. *Int Rev Neurobiol* 50:37–57. [https://doi.org/10.1016/S0074-7742\(02\)50072-6](https://doi.org/10.1016/S0074-7742(02)50072-6)
65. Roufail E, Soulis T, Boel E, Cooper ME, Rees S (1998) Depletion of nitric oxide synthase-containing neurons in the diabetic retina: reversal by aminoguanidine. *Diabetologia* 41(12):1419–1425. <https://doi.org/10.1007/s001250051087>
66. Kihara M, Schmelzer JD, Poduslo JF, Curran GL, Nickander KK, Low PA (1991) Aminoguanidine effects on nerve blood flow, vascular permeability, electrophysiology, and oxygen free radicals. *Proc Natl Acad Sci U S A* 88(14):6107–6111. <https://doi.org/10.1073/pnas.88.14.6107>
67. Kim S, Lee SY, Cho HJ (2017) Doxorubicin-wrapped zinc oxide nanoclusters for the therapy of colorectal adenocarcinoma. *Nanomaterials* 7(11):354. <https://doi.org/10.3390/nano7110354>
68. Li J, Chen H, Wang B, Cai C, Yang X, Chai Z, Feng W (2017) ZnO nanoparticles act as supportive therapy in DSS-induced ulcerative colitis in mice by maintaining gut homeostasis and activating Nrf2 signaling. *Sci Rep* 7:43126. <https://doi.org/10.1038/srep43126>
69. Casals E, Pfaller T, Duschl A, Oostingh GJ, Puentes V (2010) Time evolution of the nanoparticle protein corona. *ACS Nano* 4(7):3623–3632. <https://doi.org/10.1021/nn901372t>
70. Cedervall T, Lynch I, Foy M, Berggard T, Donnelly SC, Cagney G, Linse S, Dawson KA (2007) Detailed identification of plasma proteins adsorbed on copolymer nanoparticles. *Angew Chem* 46(30):5754–5756. <https://doi.org/10.1002/anie.200700465>
71. Lacerda SH, Park JJ, Meuse C, Pristiniski D, Becker ML, Karim A, Douglas JF (2010) Interaction of gold nanoparticles with common human blood proteins. *ACS Nano* 4(1):365–379. <https://doi.org/10.1021/nn9011187>
72. Ge C, Du J, Zhao L, Wang L, Liu Y, Li D, Yang Y, Zhou R et al (2011) Binding of blood proteins to carbon nanotubes reduces cytotoxicity. *Proc Natl Acad Sci U S A* 108(41):16968–16973. <https://doi.org/10.1073/pnas.1105270108>
73. Bhogale A, Patel N, Sarpotdar P, Mariam J, Dongre PM, Miotello A, Kothari DC (2013) Systematic investigation on the interaction of bovine serum albumin with ZnO nanoparticles using fluorescence spectroscopy. *Colloids Surf B: Biointerfaces* 102:257–264. <https://doi.org/10.1016/j.colsurfb.2012.08.023>
74. Liu S, Sui Y, Guo K, Yin Z, Gao X (2012) Spectroscopic study on the interaction of pristine C60 and serum albumins in solution. *Nanoscale Res Lett* 7(1):433. <https://doi.org/10.1186/1556-276X-7-433>
75. Bardhan M, Mandal G, Ganguly T (2009) Steady state, time resolved, and circular dichroism spectroscopic studies to reveal the nature of interactions of zinc oxide nanoparticles with transport protein bovine serum albumin and to monitor the possible protein conformational changes. *J Appl Phys* 106:034701
76. Simsikova M, Antalík M (2013) Interaction of cytochrome c with zinc oxide nanoparticles. *Colloids Surf B: Biointerfaces* 103:630–634. <https://doi.org/10.1016/j.colsurfb.2012.10.058>
77. Turci F, Ghibaudi E, Colonna M, Boscolo B, Fenoglio I, Fubini B (2010) An integrated approach to the study of the interaction between proteins and nanoparticles. *Langmuir: ACS J Surf Colloids* 26(11):8336–8346. <https://doi.org/10.1021/la904758j>
78. Wangoo N, Suri CR, Shekhawat G (2008) Interaction of gold nanoparticles with protein: a spectroscopic study to monitor protein conformational changes. *Appl Phys Lett* 92(13):133104. <https://doi.org/10.1063/1.2902302>
79. Antony SM, Han IY, Rieck JR, Dawson PL (2000) Antioxidative effect of maillard reaction products formed from honey at different reaction times. *J Agric Food Chem* 48(9):3985–3989. <https://doi.org/10.1021/jf000305x>
80. Ashoor SH, Zent JB (1984) Maillard browning of common amino acids and sugars. *J Food Sci* 49(4):1206–1207. <https://doi.org/10.1111/j.1365-2621.1984.tb10432.x>
81. Echavarria AP, Pagán J, Ibarz A (2013) Antioxidant activity of the melanoidin fractions formed from D-glucose and D-fructose with L-asparagine in the Maillard reaction. *Sci Agropecuaria* 4(1):45–54
82. Wong KH, Aziz SA, Mohamed S (2008) Sensory aroma from Maillard reaction of individual and combinations of amino acids with glucose in acidic conditions. *Int J Food Sci Technol* 43(9):1512–1519. <https://doi.org/10.1111/j.1365-2621.2006.01445.x>
83. El-Ghorab AH, Ashraf IF, Mohamed AF, Shaaban HA, El-massry KF, Farouk A (2010) The effect of pH on flavor formation and antioxidant activity of amino acids and sugars interaction products. *J Arab Soc Med Res* 5:131–139
84. Ajandouz EH, Puigserver A (1999) Nonenzymatic browning reaction of essential amino acids: effect of pH on caramelization and Maillard reaction kinetics. *J Agric Food Chem* 47(5):1786–1793. <https://doi.org/10.1021/jf980928z>
85. Tian L, Lin B, Wu L, Li K, Liu H, Yan J, Liu X, Xi Z (2015) Neurotoxicity induced by zinc oxide nanoparticles: age-related differences and interaction. *Sci Rep* 5(1):16117. <https://doi.org/10.1038/srep16117>
86. Wei L, Wang J, Chen A, Liu J, Feng X, Shao L (2017) Involvement of PINK1/parkin-mediated mitophagy in ZnO nanoparticle-induced toxicity in BV-2 cells. *Int J Nanomedicine* 12:1891–1903. <https://doi.org/10.2147/IJN.S129375>
87. Sruthi S, Millot N, Mohanan PV (2017) Zinc oxide nanoparticles mediated cytotoxicity, mitochondrial membrane potential and level of antioxidants in presence of melatonin. *Int J Biol Macromol* 103:808–818. <https://doi.org/10.1016/j.ijbiomac.2017.05.088>
88. Buzea C, Pacheco II, Robbie K (2007) Nanomaterials and nanoparticles: sources and toxicity. *Biointerphases* 2(4):MR17–MR71. <https://doi.org/10.1116/1.2815690>
89. Wang B, Feng WY, Wang TC, Jia G, Wang M, Shi JW, Zhang F, Zhao YL et al (2006) Acute toxicity of nano- and micro-scale zinc powder in healthy adult mice. *Toxicol Lett* 161(2):115–123. <https://doi.org/10.1016/j.toxlet.2005.08.007>
90. Wang L, Wang L, Ding W, Zhang F (2010) Acute toxicity of ferric oxide and zinc oxide nanoparticles in rats. *J Nanosci Nanotechnol* 10(12):8617–8624. <https://doi.org/10.1166/jnn.2010.2483>
91. Gao L, Yang ST, Li S, Meng Y, Wang H, Lei H (2013) Acute toxicity of zinc oxide nanoparticles to the rat olfactory system after intranasal instillation. *J Appl Toxicol: JAT* 33(10):1079–1088. <https://doi.org/10.1002/jat.2842>
92. Hackenberg S, Scherzed A, Technau A, Kessler M, Froelich K, Ginzkey C, Koehler C, Burghartz M et al (2011) Cytotoxic, genotoxic and pro-inflammatory effects of zinc oxide nanoparticles in human nasal mucosa cells in vitro. *Toxicol In Vitro* 25(3):657–663. <https://doi.org/10.1016/j.tiv.2011.01.003>

93. Doak SH, Manshian B, Jenkins GJ, Singh N (2012) In vitro genotoxicity testing strategy for nanomaterials and the adaptation of current OECD guidelines. *Mutat Res* 745(1–2):104–111. <https://doi.org/10.1016/j.mrgentox.2011.09.013>
94. Gurr JR, Wang AS, Chen CH, Jan KY (2005) Ultrafine titanium dioxide particles in the absence of photoactivation can induce oxidative damage to human bronchial epithelial cells. *Toxicology* 213(1–2):66–73. <https://doi.org/10.1016/j.tox.2005.05.007>
95. Pan Y, Leifert A, Ruau D, Neuss S, Bornemann J, Schmid G, Brandau W, Simon U et al (2009) Gold nanoparticles of diameter 1.4 nm trigger necrosis by oxidative stress and mitochondrial damage. *Small* 5(18):2067–2076. <https://doi.org/10.1002/sml.200900466>
96. Carlson C, Hussain SM, Schrand AM, Braydich-Stolle LK, Hess KL, Jones RL, Schlager JJ (2008) Unique cellular interaction of silver nanoparticles: size-dependent generation of reactive oxygen species. *J Phys Chem B* 112(43):13608–13619. <https://doi.org/10.1021/jp712087m>
97. Long TC, Saleh N, Tilton RD, Lowry GV, Veronesi B (2006) Titanium dioxide (P25) produces reactive oxygen species in immortalized brain microglia (BV2): implications for nanoparticle neurotoxicity. *Environ Sci Technol* 40(14):4346–4352. <https://doi.org/10.1021/es060589n>
98. Wang Y, Aker WG, Hwang HM, Yedjou CG, Yu H, Tchounwou PB (2011) A study of the mechanism of in vitro cytotoxicity of metal oxide nanoparticles using catfish primary hepatocytes and human HepG2 cells. *Sci Total Environ* 409(22):4753–4762. <https://doi.org/10.1016/j.scitotenv.2011.07.039>
99. Hussain SM, Hess KL, Gearhart JM, Geiss KT, Schlager JJ (2005) In vitro toxicity of nanoparticles in BRL 3A rat liver cells. *Toxicol In Vitro* 19(7):975–983. <https://doi.org/10.1016/j.tiv.2005.06.034>
100. Hu X, Cheng W, Wang T, Wang E, Dong S (2005) Well-ordered end-to-end linkage of gold nanorods. *Nanotechnology* 16(10):2164–2169. <https://doi.org/10.1088/0957-4484/16/10/032>
101. Aliev G, Daza J, Herrera AS, del Carmen Arias Esparza M, Morales L, Echeverria V, Bachurin SO, Barreto GE (2015) Nanoparticles as alternative strategies for drug delivery to the Alzheimer brain: electron microscopy ultrastructural analysis. *CNS Neurol Disord Drug Targets* 14(9):1235–1242. <https://doi.org/10.2174/1871527314666150821102631>